

Galactic archaeology: IMF and depletion in the “thin disk”

K.-P. Schröder^{1,2*}, B. Pagel¹

¹*Astronomy Centre, CPES, University of Sussex, Falmer, Brighton BN1 9QJ, UK*

²*Technische Universität Berlin, Zentrum für Astronomie und Astrophysik, PN 8-1, Hardenbergstr. 36, 10623 Berlin, Germany*

Received Feb. 3, 2003; accepted ..., 2003

ABSTRACT

We determine the initial mass function (IMF) of the “thin disk” by means of a direct comparison between synthetic stellar samples (for different matching choices of IMF, star formation rate SFR and depletion) and a complete (volume-limited) sample of single stars near the galactic plane ($|z| < 25$ pc), selected from the Hipparcos catalogue ($d < 100$ pc, $M_V < +4.0$). Our synthetic samples are computed from first principles: stars are created with a random distribution of mass M_* and age t_* which follow a given (genuine) IMF and $SFR(t_*)$. They are then placed in the HR diagram by means of a grid of empirically well-tested evolution tracks. The quality of the match (synthetic versus observed sample) is assessed by means of star counts in specific regions in the HR diagram. 7 regions are located along the MS (main sequence, mass sensitive), while 4 regions represent different evolved (age-sensitive) stages of the stars.

We find a bent slope of the IMF (using the Scalo notation, i.e., power law on a logarithmic mass scale), with $\Gamma_1 = -1.70 \pm 0.1$ (for $1.1M_\odot < M_* < 1.6M_\odot$) and $\Gamma_2 = -2.1 \pm 0.1$ (for $\approx 4M_\odot > M_* > 1.6M_\odot$). In addition, comparison of the observed MS star counts with those of synthetic samples with a different prescription of the MS core overshooting reveals sensitively that the right overshoot onset is at $M_* = 1.50M_\odot$.

The counts of evolved stars, in particular, give valuable evidence of the history of the “thin disk” (apparent) star formation and lift the ambiguities in models restricted to MS star counts. A match of the evolved star counts yields a stellar depletion in the sample volume which increases with age (i.e., by apparent $SFR(\text{age}) / SFR_0$). A very good match is achieved with a simplistic diffusion approximation, with an age-independent diffusion time-scale of $\tau_{\text{dif}} = 6.3 \cdot 10^9$ yrs and a (local) $SFR_0 = 2.0 \pm 0.1$ stars (with $M_* > 0.9M_\odot$) formed per 1000 years and (kpc)³. We also discuss this “thin disk” depletion in terms of a geometrical dilution of the expanding stellar “gas”, with $H_z(t_*) \propto \sigma_W(t_*)$. This model applies to all stars old enough to have reached thermalization, i.e. for $t_* > 7 \cdot 10^8$ yrs and $H_z > 230$ pc. It yields a column-integrated (non-local) “thin-disk” SFR_{col} which has not changed much over time ($< 30\%$), $SFR_{\text{col}} \approx 0.82 \text{ pc}^{-2} \text{ Gyr}^{-1}$ (i.e., stars with $M_* > 0.9M_\odot$).

Key words: Stars: evolution – Stars: late-type – Stars: mass function – Galaxy: kinematics and dynamics – Galaxy: disk – Solar neighbourhood

1 INTRODUCTION

The case of the IMF has spurred a vast amount of literature over the past 3 decades. We would like to mention only the classic work and reviews by Miller & Scalo (1979) and Scalo (1986), together with Scalo (1998) and Kroupa (2001) for reference to the more recent work in the field. The classical approach to derive the IMF of field stars in the galactic disk follows a line of steps: (i) derive the stellar distribution in absolute magnitude from the observed distribution in apparent

magnitude, requiring the respective vertical space-density scale-height, and convert that into the luminosity function LF for MS stars, (ii) apply a theoretical mass-luminosity (m-L) relationship for obtaining the present-day mass function (PDMF), and (iii) model the IMF on the PDMF, for a given SFR history. As discussed by Scalo (1998), each of these steps introduces specific uncertainties so that the case of the IMF is far from being closed. Scalo (1998) and Kroupa (2001) even argue that there are systematic variations in the IMF, especially between the field star IMF and the various IMF’s derived from galactic stellar clusters.

The availability of good parallaxes, as required for a precise field star LF, is mutually exclusive with the neces-

* E-mail: kps@star.cpes.sussex.ac.uk

sity of a large stellar sample. Therefore, early work on the LF had to rely on a statistical approach, based on the apparent magnitudes, or on photometric parallaxes (e.g., Gilmore & Reid 1983). These approaches link the question of the IMF to that of the spatial stellar distribution, i.e., perpendicular to the galactic plane. Most notably, Gilmore & Reid (1983) found that (i) the stellar spatial density scale heights increase with lower masses, and that (ii) the global spatial distribution could be described by a (denser) Galactic “thin disk” plus an extended Galactic “thick disk”. Especially the first point is of importance when deriving a field star IMF, as we will show below.

The great interest in the IMF is fuelled not only by the attempts to understand and model the star formation process(es). Finding the IMF is also closely linked to the question of galactic star formation history, i.e., whether and how the SFR has varied over time. Both IMF and SFR(t) are important ingredients of galaxy models since these quantities determine such important aspects as the chemical evolution and the luminosity evolution of a galaxy (see, e.g., Dwek 1998, Gilmore 1999, Hensler 1999, Pagel 2001a,b). Furthermore, the IMF of more massive stars is of particular interest for the formation of star-burst regions and stellar clusters, and for the evolution of young galaxies. Our Galaxy would make an ideal test case for detailed galaxy evolution models, if we could determine the IMF and SFR(t) with sufficient accuracy. Already, we have quite a good account of the stellar population(s), the (local) kinematics and chemical composition as a function of age.

A general problem in this context is the inherent ambiguity of any interpretation that is restricted to MS stars: Towards lower stellar masses, the mean age of a MS star increases accordingly. Consequently, assuming a different time-dependence of the rate of star formation (i.e., increasing, or decreasing with age) has the same effect on the expected numbers of stars on the lower MS as changing the IMF accordingly. This degeneracy of SFR(t) and lower IMF (see, e.g., Binney et al. 2000) allows a variety of false combinations of IMF and SFR(t) to match the PDMF of MS stars. It is therefore important to lift this degeneracy by extracting additional, specifically age-sensitive information from the HR diagram which is buried in the properties and numbers of the evolved stars.

Matters are further complicated by the galactic disk dynamics. Relevant properties of the star formation process are the genuine IMF and SFR at the time of the star formation and in a defined volume on the galactic plane – i.e., within the vertical extent of the star formation sites. However, present-day counts of stars in a solar neighbourhood volume translate into an *apparent* SFR which decreases towards larger age (Schröder & Sedlmayr 2001). This depletion of stars in the galactic plane is caused by a dilution of the “heated stellar gas” which is expanding vertically (see below). If not accounted for, this effect would make a spurious, systematic difference to, e.g., the steepness of any IMF derived from a volume-limited stellar sample. Consequently, the above-mentioned classical studies of IMF and SFR have used the invariant column-integrals. Their dependence on stellar mass and age is equivalent to that of the genuine IMF and the depletion-corrected SFR in the volume. This column-integral approach, however, has the disadvantage of being no more accurate than the required and presently

quite limited knowledge of space-density scale-heights as a function of stellar age.

For this reason, we use the direct approach to star formation, based on the stellar records in a well-defined (local) volume, and an interpretation in terms of a matching synthetic sample. Synthetic stars are randomly placed in a well-tested evolution grid, and their numbers are (statistically) defined by the given (genuine) IMF and (apparent) SFR_{ap} in the volume. In previous studies we have shown that counts of specific synthetic stars compare well with the respective, observed present-day star counts (Schröder 1998; Schröder & Sedlmayr 2001). The potential of this approach lies in its simplicity. We do not need to determine a LF, nor to use a (m-L) relation – this is automatically accounted for by our synthetic sample creation, as is the mass-dependent fraction of post-AGB stars which are left out by a MS-based PDMF. The genuine SFR(t) in the volume is then derived from a depletion description (see below), for which a maximum of age-sensitive information is derived from the stellar sample.

Studies based on a similar approach have been undertaken by Bertelli & Nasi (2001), who, in addition, account for a variety of metallicity (see also Bertelli et al. 1992), and by Binney et al. (2000). However, these authors did not exploit the specific, age-sensitive information provided by the counts of evolved stars. In fact, the models of Bertelli & Nasi (2001) show an excess of the number of evolved stars by (relative to the MS stars of same initial mass) a factor of 1.5, while the problem of stellar diffusion away from the galactic plane has not been addressed.

Consequently, the work presented here pays special attention to three points which appear crucial for an improvement over previous work: (1) In section 2, we describe a large, volume-limited sample of stars from the Hipparcos catalogue, which we selected for good proximity to the galactic plane ($|z| < 25$ pc) in order to avoid any selective under-representation of young, massive stars at larger $|z|$. (2) In section 3, we study the stellar depletion in the galactic plane. A simplistic but well-matching diffusion approximation with an age-independent diffusion time is compared with a more physical model. The latter describes the depletion in terms of geometrical dilution caused by the stellar kinematics: stars old enough ($t_* > 7 \cdot 10^8$ yrs) to have “thermalized” are expanding to larger scale heights exactly as their vertical velocity distribution increases with age. We find a semi-empirical prescription of the stellar space-density scale-heights in agreement with the available observational evidence. (3) In section 4, we describe the computation of our synthetic samples and how we assess a match with the observed stellar sample. Special consideration is given to the counts of evolved stars, in order to constrain the right choice of IMF, SFR(t) and depletion as well as possible.

2 COMPLETE SAMPLES OF SINGLE STARS ON AND NEAR THE GALACTIC PLANE

In principle, we use the same volume-limited (i.e., $d < 100$ pc) sample of single stars, based on the Hipparcos catalogue, as for earlier work (Schröder 1998), but solving the problem with consistency: In comparison to the very local sample with $d < 50$ pc (used in Schröder & Sedlmayr, 2001), the 100pc-volume provides a comfortably larger statistical

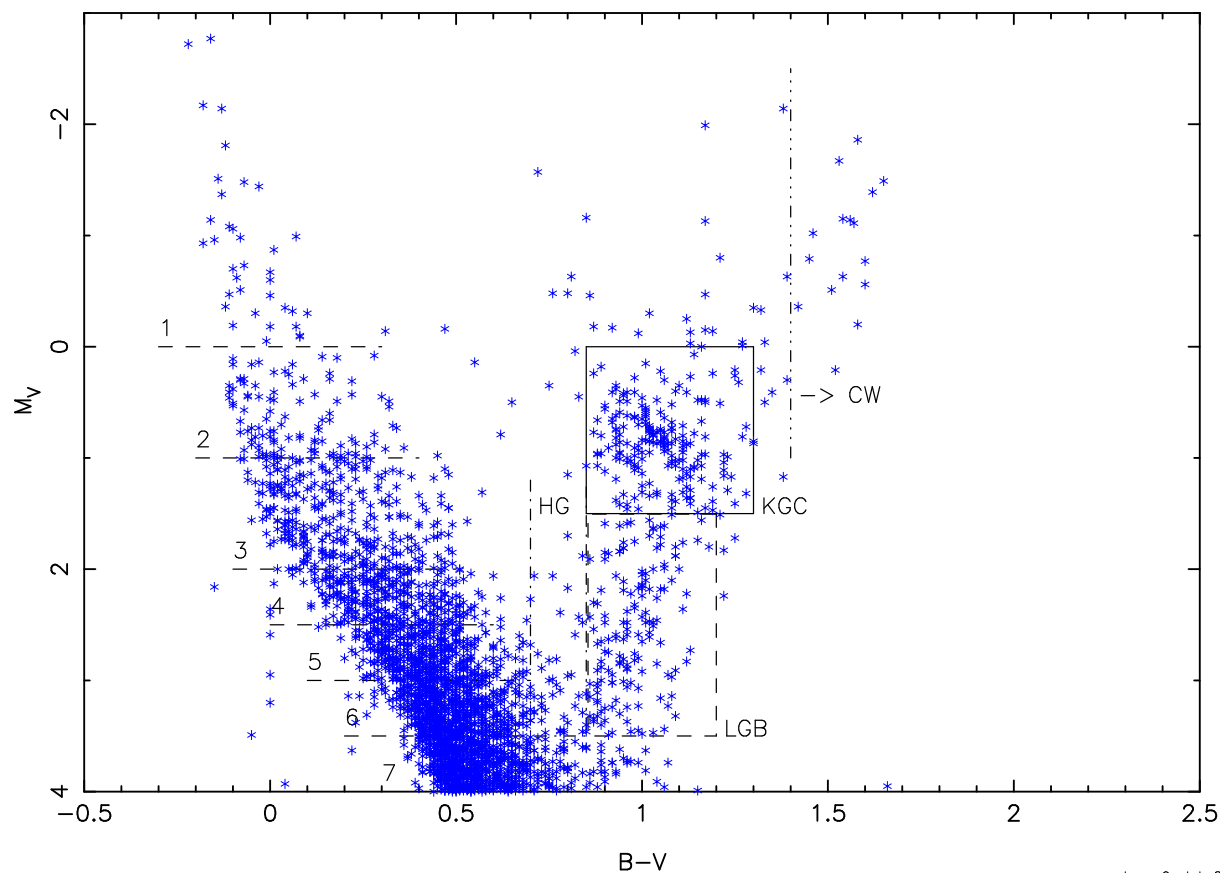


Figure 1. The observed HR diagram of all single stars which are within 25 pc to the galactic plane, less than 100 pc away, and brighter than $M_V = 4.0$, as obtained from the Hipparcos catalogue entries. Also shown are the regions used for characteristic star counts (see text), 7 along the main sequence and 4 for evolved stages.

stellar basis, but it also comprises larger distances z from the galactic plane which already make a difference to the PDMF of massive stars. Therefore, this investigation now discriminates against all stars with $|z| > 25\text{pc}$ within 100 pc, which still leaves us with larger, statistically more significant star counts than from the 50pc-sample. Star counts from neighbouring space are used, where possible, to derive space-density scale-heights for specific groups of stars (see Table 1).

For computing the z values, we adopted an offset of the Sun of 15pc north of the galactic plane (Cohen 1995), which intersects the spherical sample volume around the Sun ($R = 100\text{pc}$, $V = 4.19 \cdot 10^6\text{pc}^3$) off-centre. In order to keep the star counts of the neighbouring space reasonably large, we divide the spherical volume into slabs of (A) all stars within $|z| < 25\text{pc}$ ($V_A = 1.50 \cdot 10^6\text{pc}^3$), (B) all stars between $25\text{pc} < |z| < 50\text{pc}$ ($V_B = 1.31 \cdot 10^6\text{pc}^3$), and (C) those stars in the polar sections of the 100pc sphere, up to $|z| < 85\text{pc}$ and 115pc, respectively ($V_C = 1.38 \cdot 10^6\text{pc}^3$).

Stellar population densities in the HR diagram are assessed by means of star counts in 7 regions along the main sequence (MS1 to MS7, sensitive to the initial mass function IMF), and in 4 regions representative of different evolutionary stages and stellar ages, containing information on the star formation history $\text{SFR}(t_*)$ and the diffusion losses over time: the Herzsprung gap (HG), the K giant clump (KGC),

the lower giant branch (LGB) and stars with cool winds (CW), with border-lines as shown in Fig. 1. The observed HG counts are particularly affected by any unrecognized binaries with a composite colour and must be considered as upper limits, only.

Since the Hipparcos catalogue is complete at least for stars brighter than $V = 7.3$ (in some regions of the sky even down to $V = 9$, see Perryman et al. 1997), completeness of volume-limited samples is automatically given for all stars within 50pc which are brighter than $M_V = 4$. Towards 100pc distance, however, star counts of regions MS6 and MS7 (with $M_V = 3.0$ to 4.0) would be somewhat incomplete. By applying the (unaffected) star count ratios in the 50pc sample (as from Schröder & Sedlmayr 2001), especially to MS6, MS7 and the total number of stars (TN) as a multiple of MS5, we can make a good estimate of the missing fractions. For the stars within $|z| < 25\text{pc}$ of the galactic plane, we find corrections for the counts of MS6 by 4%, of MS7 by 25%, and of TN by 8%. These figures need to be added for a comparison with the synthetic samples discussed in section 4.

Normalizing the characteristic star counts to their respective volumes (A, B and C as given above), we derive approximate, local scale heights, as listed in the bottom line of Table 1. In order to handle any intrinsic fluctuations of the star counts, we applied a comparison of the ratios $N_{*,A}/N_{*,B}$ and $N_{*,A}/N_{*,C}$ with volume integrals over exponential den-

Table 1. Characteristic star counts in the space slabs A, B and C, for different regions in the HR diagram along the main sequence (MS) and for different groups of evolved stars (see Fig. 1 and text). The bottom line gives the approximate scale heights of the respective stellar number densities.

Sample	z [pc]	MS1	MS2	MS3	MS4	MS5	MS6	MS7	TN	HG	KGC	LGB	CW
A	[0–25]	38	106	317	327	484	712	850	3348	< 49	205	157	16
B	[25–50]	13	79	227	261	365	581	743	2736	< 53	171	146	21
C	[50–115]	20	63	212	260	374	644	835	2921	< 69	175	156	22
	$H_{z,*} \approx$	60:	135	160	320:	270:	> 400	—	> 400	—	> 400	—	—

sity distributions for different scale heights. For the sake of a more realistic description, we assume a constant space-density around the galactic plane for $|z| < 10$ pc.

The small space-density scale-heights of the stars in groups MS1 to MS3 confirm that the young and more massive stars are much more concentrated to the galactic plane, and that their correct assessment requires a volume restriction in z . For MS6, MS7 and LGB, in fact, stellar number densities increase slightly from B to C. This local deficiency of stars appears to correspond with the low- z -structure found by Kuiken & Gilmore (1989). Hence, the H_z -values stated in Table 1 should be larger than what is typical for the galactic thin disk over a larger z -range. Clearly, a complete sample covering a larger volume, as will be available from the future GAIA (e.g., Perryman 2002) and DIVA (Bastian et al. 1996, Seifert et al. 1998) missions, is highly desirable.

3 VERTICAL SPACE DENSITY STRUCTURE AND “THIN DISK” DYNAMICS

A lot of observational work has been done on the *stellar space-density scale-heights* H_z vertical to the galactic plane. Galactic structure studies on a wide range of stars have come up with the concept of a “thin” disk and an old “thick” disk, with scale heights of ≈ 250 pc to 400 pc (thin disk, e.g., Gilmore & Reid 1983, Kent et al. 1991, Ojha et al. 1996, Siebert et al. 2002) versus 700 pc to 800 pc (thick disk, e.g., Ojha et al. 1999, Robin et al. 1996, Kerber et al. 2001, Phleps et al. 2000). However, a single scale height does not describe the “thin disk” stellar distribution adequately. Rather, each particular class of stars has a different scale height which increases with the respective mean stellar age. Evidence comes from selective star counts which focus on narrow age ranges, though specific values may still be quite uncertain:

(i) From an interstellar extinction study, Vergely et al. (1998) find a scale-height of the local ISM density and clouds, the regions of star formation, to be between 35 pc and 55 pc.

(ii) For young and massive stars, scale-heights between 25 pc and 65 pc have been found (Reed 2000, for OB stars), as well as 45 pc (Conti & Vacca 1990, WR stars).

(iii) From a study of all F-type stars within a distance of 50 pc, which (on average) are half-way through their main-sequence life, Marsakov & Shelevyev (1995) find a scale-height of 160 pc.

(iv) For thin disk K dwarfs, Kuiken & Gilmore (1989) find a scale-height of 249 pc for $z > 300$ pc. Nearer to the galactic plane, their density data show pronounced low- z -

structure. A rough average would yield a significantly larger scale-height.

(v) For the galactic disk subgiants, Mendez & van Altena (1996) find a red-giant scale-height of 250 pc. Many of these are He-burning K-giant-clump stars, represented by our group KGC.

(vi) Jura & Kleinmann (1992a, b) studied K and M-type (O-rich) variable AGB stars and Miras. For periods of $P = 300\text{--}400$ days, indicative of a larger luminosity and, hence, less small mass (around 1.1, possibly 1.2 M_\odot) and lesser age, they find a typical scale-height of 250 pc.

(vii) For the supposedly less luminous, and therefore presumably slightly older group of stars with $P = 200\text{--}300$ days, the same authors estimate 500 pc. In addition, Jura (1994) finds a scale-height of 600 pc for the O-rich, short-period Miras, which he estimates at a mass as small as about $1.0M_\odot$.

(viii) for RR Lyrae stars with a moderate metal underabundance ($[\text{Fe}/\text{H}] > -1$) Layden & Andrew (1995) find a scale height of 700 pc. As expected from their abundance, this places them at the transition from thin to thick disk.

A similar range of scale-heights emerges from a study of LMC foreground stars, grouped by different spectral class and metallicity, by Oestreicher & Schmidt-Kaler (1995). These authors find 105 pc for early-type stars, to over 500 pc for the metal-poor, late-type giants.

In line with these observations, an analytical description of the stellar dynamics suggests age-dependent scale heights which increase in proportion with the vertical stellar velocity distribution σ_w :

After a few oscillations at right angles to the Galactic plane, stars reach a state of dynamical equilibrium governed by the potential gradient at right angles to the plane and by the velocity dispersion (Oort 1932). With the progress of time, the velocity dispersion increases from the effect of encounters with interstellar clouds; alternatively, the oldest stars, belonging to the Thick Disk, are born with a high velocity dispersion, which they still retain, either as a result of being born from collapsing gas clouds that had not yet undergone complete dissipation of their potential energy (Eggen, Lynden-Bell & Sandage 1962; Burkert, Truran & Hensler 1992), or because of merger events in the early history of the disk (Robin et al. 1996; Pilyugin 1996). Either way, the velocity dispersion increases with age (Wielen 1977; Lacey 1984; Sommer-Larsen & Antonuccio-Delogu 1993) resulting in an increase in the width of the density distribution as a function of z .

By Jeans’s theorem, the distribution function in phase space in a steady state is a function of isolating integrals of the motion (Jeans 1915, Lynden-Bell 1962). In the approx-

imation where z -motions are considered as uncoupled from motion in the plane, the only isolating integral is the vertical energy

$$E = \frac{1}{2}w^2 + \phi \quad (1)$$

and the distribution function (assumed to be gaussian for an isothermal stellar population) is

$$f(z, w) = \nu(z) \frac{1}{\sigma_w \sqrt{2\pi}} e^{-(w^2 + 2\phi)/2\sigma_w^2} \quad (2)$$

where ν is the volume density at height z , w the velocity along the z -axis and σ_w the corresponding velocity dispersion. Consequently the total volume density is

$$\nu(z) = \int_{-\infty}^{\infty} f(z, w) dw = \nu(0) e^{-\phi/\sigma_w^2}. \quad (3)$$

Kuijken & Gilmore (1989) have given an expression for $\phi(z)$:

$$\phi = 2\pi G [\Sigma_0 (\sqrt{z^2 + D^2} - D) + \rho_{\text{eff}} z^2], \quad (4)$$

where Σ_0 is the mass surface density of the disk, D a length scale defining the transition from the linear regime $K_z \propto z$ to $K_z = \text{const.}$ and ρ_{eff} is the contribution of the dark halo to the local density of gravitating matter. This expression can be expanded (for $z^2 < D^2$) as a binomial series

$$\begin{aligned} \phi &\simeq 2\pi G \left[\Sigma_0 D \left(\frac{1}{2} \frac{z^2}{D^2} - \frac{1}{8} \frac{z^4}{D^4} + \dots \right) + \rho_{\text{eff}} z^2 \right] \\ &= 2\pi G \left[\left(\frac{\Sigma_0}{2D} + \rho_{\text{eff}} \right) z^2 - \frac{1}{8} \Sigma_0 D \left(\frac{z}{D} \right)^4 + \dots \right]. \end{aligned} \quad (5)$$

The first term, $\phi \propto z^2$, corresponds to simple harmonic motion where from Eq 3,

$$\frac{\nu(z)}{\nu(0)} = e^{-A^2 z^2 / \sigma_w^2}, \quad (6)$$

where

$$A^2 \equiv 2\pi G \left(\frac{\Sigma_0}{2D} + \rho_{\text{eff}} \right) \quad (7)$$

and in this approximation the column density of a tracer population by number is related to the central density by

$$N = \int_{-\infty}^{\infty} \nu(z) dz = \nu(0) \frac{\sigma_w}{A} \sqrt{\pi}, \quad (8)$$

or

$$\nu(0) = \frac{A}{\sigma_w \sqrt{\pi}} N, \quad (9)$$

i.e. we have a gaussian distribution with an effective scale height proportional to σ_w ; in a higher approximation to $\phi(z)$, Eq (3) must be integrated over z numerically.

The values of the parameters Σ_0 , D and ρ_{eff} have been discussed by Kuijken & Gilmore (1989) and very recently

by Siebert, Bienaymé and Soubiran (2002), among others. Σ_0/D is rather well determined at $0.18 M_{\odot} \text{ pc}^{-3}$ and $\rho_{\text{eff}} \simeq 0.02$ is a relatively small correction, but there is a degeneracy in the determination of Σ_0 and D . Siebert et al. favour $D \approx 400$ pc, by contrast to Kuijken & Gilmore’s value of only 180 pc. The difference is crucial to the range of validity of Eqs 6, 8 and 9. Taking $D = 500$ pc, the quadratic approximation to ϕ is accurate to better than 10 per cent up to $z = 350$ pc, which would make it applicable to virtually all thin-disk stars in our neighbourhood, whereas with $D = 180$ pc, the situation would be very different. The actual scale heights of the more numerous, less massive stars presented above, however, suggest that the approximation is indeed valid for our sample.

In the approximation of the density distribution $\nu(z)$ being an exponential function of z with a scale height H_z , we have the simple relation $N = 2 \cdot H_z \cdot \nu(0)$. In combination with Eq (9) it then follows that $H_z(t_*)$ expands $\propto \sigma_w(t_*)$ and $\nu(0)$ dilutes $\propto 1/\sigma_w(t_*)$ with age and increasing vertical velocity dispersion.

For $\sigma_w(t_*)$ as a function of stellar age, we take the simple (constant-diffusion) solution of Wielen (1977), $\sigma_w = (a_W + b_W \cdot t_*)^{0.5}$. For $t_* > 7 \cdot 10^8$ yrs, we find that Wielen’s empirical data points, as well as those of Sommer-Larsen & Antonuccio-Delogu (1993), can be well enough represented by $a_W = 72 \text{ (km/s)}^2$, $b_W = 72 \text{ (km/s)}^2/10^9 \text{ yrs}$.

Finally, with $H_z \propto \sigma_w(t_*)$ and in consideration of the above listed empirical stellar space density scale heights, we have adopted the following prescription (in pc) as a function of age (in yrs):

$$H_{z,*} = 177 \cdot (1.0 + t_*/10^9)^{0.5}, \quad t_* > 7 \cdot 10^8 \quad (10)$$

In particular, scale heights range from around 265 pc (about the average half-thickness of the thin disk according to Ojha et al. 1996, reached around an age of $t_* \approx 1.2 \cdot 10^9$ yrs) to about 560 pc for the very oldest ($9 \cdot 10^9$ yrs) thin-disk stars.

The present-day, young stars are formed very near the galactic plane, with the scale-height of the ISM clouds ($H_{z,0} \approx 45$ pc, see above), and drift away with increasing age. As long as their kinematics are not thermalized (for $t_* < 7 \cdot 10^8$, $H_z < 230$ pc), we prescribe their scale-heights mainly by a quadratic superposition of the initial scale-height $H_{z,0}$ and a term which is linear in age (in years), as:

$$H_{z,*} = (45^2 + (t_*/3.105 \cdot 10^6 \text{ yrs})^2)^{0.5}, \quad t_* < 7 \cdot 10^8 \quad (11)$$

The resulting values are in reasonable agreement with the scale-heights obtained directly from the corresponding age-groups of Hipparcos stars (i.e., MS1, MS2, and MS3 in Table 1).

4 “THIN DISK” DEPLETION BY DILUTION: EXPANSION OF THE STELLAR “GAS”

Near the galactic plane, the vertical gravitational net force is small enough to be neglected. In an earlier study (Schröder & Sedlmayr 2001), we therefore suggested a very simplistic

model in which depletion was prescribed as a diffusion effect, with a single diffusion-time scale τ_{diff} for all stars (now referred to as model a). A value of $6.3 \cdot 10^9$ yrs, which we here confirm to give a good match of the observed star counts, leads to a 50% depletion of stars aged $4 \cdot 10^9$ yrs. To give another example of the significance of this depletion: the ratio of less massive giant stars (aged around $5 \cdot 10^9$ yrs) over their MS counterparts (of average age $2.4 \cdot 10^9$ yrs) is reduced by a factor of 1.5 (which is of the order of the mismatch found with synthetic samples by Bertelli & Nasi, 2001).

For the IMF, we use the conventional power-law notation (Scalo, 1986) that counts on a logarithmic mass scale:

$$\text{IMF}(M_*) = dn_*/d \log M_* \propto M_*^\Gamma \quad (12)$$

To allow for a bent slope, we use a Γ_1 for masses smaller than $1.6M_\odot$, and a Γ_2 for larger masses. The mass-range of this study is limited by the observed sample to about (effectively) $4M_\odot$ at the upper, and to about $1.1M_\odot$ at the lower end.

Our principal star formation observable is the *apparent* $\text{SFR}_{\text{ap}}(t_*)$ in the sample volume. As mentioned before, it appears to have been much lower in the past than at present (SFR_0) due to a dilution effect of the expanding stellar “gas”. Therefore, we introduce a depletion factor of $F_{\text{depl}}(t_*) = \text{SFR}_{\text{ap}}(t_*)/\text{SFR}(t_*)$ relative to the genuine star formation rate $\text{SFR}(t_*)$ in the volume, at the time of the star formation. In addition, we consider possible slow changes in the genuine SFR by an exponential factor, relative to the present-day star formation rate SFR_0 , defined on the reversed time-scale of the stellar age t_* (in years):

$$\text{SFR}_{\text{ap}}(t_*) = F_{\text{depl}}(t_*) \cdot \text{SFR}_0 \cdot e^{\gamma t_*/10^9} \quad (13)$$

Our values of the SFR (in the volume) are given in stars formed per year which have a mass larger than $0.9M_\odot$, in the local sample volume A (see previous section) of $1.5 \cdot 10^6 \text{pc}^3$. For our simplistic diffusion model (a), the depletion factor F_{depl} (for any given number n_* of similar stars of a specific age and mass) is itself a t_* -dependent, exponential term (in Schröder & Sedlmayr 2001, both these terms were simply merged into one).

A more physical description of the depletion is given in terms of a geometrical dilution of stellar space density into the column (model b). According to Eq 9, the depletion factor is then proportional to the vertical velocity distribution or, equally, to the scale-height of a group of stars of a given age:

$$F_{\text{depl}}(t_*) = H_{\text{ref}}/H_z(t_*) \quad (14)$$

This model (b) applies, once (1) the stellar “gas” has thermalized (i.e., if $t_* > 5 \cdot 10^8$ yrs or more), and (2) if the depletion by dilution into the column is not compensated for by any fill-in from radial mixing in the disk. However, for the past $7 \cdot 10^8$ yrs, significant fill-in is evident: From this more recent time-span we would expect a dilution by a factor of about 5 (from the scale-height of the star-formation layer, about 45 pc, to $H_z(t_* = 7 \cdot 10^8) = 230$ pc. Instead, the respective $F_{\text{depl}}(t_*)$ required by a matching synthetic sample (see below) is about 0.85 or even closer to 1.

To match this depletion at the onset of geometrical dilution ($7 \cdot 10^8$ yrs), H_{ref} must be 195 pc. For all younger ($t_* <$

$7 \cdot 10^8$ yrs) stars we use the simple exponential approximation of the depletion factor this time with $\tau_{\text{diff}} = 4.5 \cdot 10^9$ yrs), guided by a smooth transition with the depletion derived from dilution.

For a quite limited volume around the Sun, a significant fill-in over the more recent past must be expected: At present, it is located right in between two spiral arms. Consequently, the present-day, local SFR is much below the global, average SFR for the “thin disk”. As we look towards older stars, radial mixing changes the observed SFR from a local (for the youngest stars) to a non-local (after 2 to 3 orbital periods) quantity.

A quantity more relevant for the physics of the galactic disk is the column-integrated star formation rate, which relates to the apparent local SFR in the volume, our principal observable, by:

$$\text{SFR}_{\text{col}}(t_*) \approx 2 \cdot H_z(t_*) \cdot \text{SFR}_{\text{ap}} \quad (15)$$

This column-integrated SFR is then related to the *real* local star formation in the volume (allowing here for a possible exponential dependence on age) and the subsequent depletion, simply by:

$$\text{SFR}_{\text{col}}(t_*) \approx 2 \cdot H_z(t_*) \cdot F_{\text{depl}}(t_*) \cdot \text{SFR}_0 \cdot e^{\gamma t_*/10^9} \quad (16)$$

The $\text{SFR}_{\text{col}}(t_*)$ derived from our model first increases with look-back time (driven by the above-mentioned fill-in from radial mixing which causes scale-heights of the younger stars to increase steeply with age), until from an age of $7 \cdot 10^8$ yrs it then settles on a disk-averaged value (see below). This is about 4 times larger than that of the low present-day, interarm star formation. The same effect would be observed, if the effective star formation layer had just been more expanded in the past (as noted by Binney et al. 2000).

5 SYNTHETIC STELLAR SAMPLES AND THE IMF IN THE GALACTIC PLANE

– **The synthetic samples:** Our synthetic stellar samples are computed from first principles: stars are created with a random choice of mass M_* and age t_* within a distribution which is prescribed by the choice of IMF for stellar masses, and $\text{SFR}(t_*)$ for the ages. These synthetic stars are then placed on a fine-meshed grid of individually computed evolution tracks, in order to obtain their present-day distribution in the observational HR diagram (see also Schröder & Sedlmayr 2001). We computed the evolution tracks with a fast but well-tested code, developed by Peter Eggleton (Eggleton 1971, 1972, 1973). This code has been updated with up-to-date opacities and colour tables. Its performance and the right choice of mixing length and overshoot prescription has been tested very critically in several studies. Respective evolution models have been compared with a number of real MS and giant stars in well-observed eclipsing binaries, and isochrones have been compared with stellar cluster data (see Schröder et al. 1997, and Pols et al. 1997, 1998).

Because of the limited observational data, we did not explicitly account for the effects of a moderate range in chemical composition, which mostly contribute to a more smeared-out distribution of the stars in the synthetic HR

Table 2. Characteristic star counts N_i of different synthetic samples and their deviations from observed values, in units of the statistical variation $\sqrt{n_{i,\text{obs}}}$, plus the mean deviation $|\delta|_{\text{av}}$ (double weight is given to KGC and LGB counts). Under the best-matching, simple diffusion model, synthetic samples based on different evolution grids and thin disk ages are listed, followed by those derived with depletion by (mainly) dilution. A constant SFR ($\gamma = 0$) gives a better match than SFRs decreasing from an initially 30% ($\gamma = 0.03$) and 70% ($\gamma = 0.06$) higher value.

Model	MS1	MS2	MS3	MS4 HG	MS5 KGC	MS6 LGB	MS7 CW	$ \delta _{\text{av}}$
Obs.	38	106	317	327 (< 49)	484 205	740 157	1068 16	—
$\tau_{\text{dif}} = 6.29$	37 ^(-0.10)	109 ^(+0.29)	315 ^(-0.14)	325 ^(-0.13) 44	495 ^(+0.48) 209 ^(+0.28)	739 ^(-0.04) 149 ^(-0.61)	1077 ^(+0.27) 18 ^(+0.40)	0.30
ovo=1.8	40 ^(+0.25)	108 ^(+0.17)	317 ^(+0.0)	260 ^(-3.7) 44	472 ^(-0.50) 197 ^(-0.59)	770 ^(+1.1) 179 ^(+1.8)	1076 ^(+0.23) 20 ^(+1.0)	0.98
ovo=1.6	40 ^(+0.25)	109 ^(+0.27)	325 ^(+0.44)	311 ^(-0.87) 42	451 ^(-1.5) 206 ^(+0.11)	764 ^(+0.87) 162 ^(+0.36)	1062 ^(-0.17) 19 ^(+0.65)	0.50
ovo=1.4	37 ^(-0.13)	112 ^(+0.58)	322 ^(+0.29)	318 ^(-0.50) 39	539 ^(+2.5) 200 ^(-0.36)	751 ^(+0.41) 147 ^(-0.77)	1064 ^(-0.13) 22 ^(+1.5)	0.69
$t_{9\text{max}}10$	38 ^(-0.06)	107 ^(+0.14)	311 ^(-0.33)	330 ^(+0.19) 39	507 ^(+1.05) 199 ^(-0.39)	716 ^(-0.89) 159 ^(+0.18)	1067 ^(-0.04) 18 ^(+0.44)	0.36
$t_{9\text{max}}8$	41 ^(+0.45)	112 ^(+0.58)	317 ^(-0.02)	324 ^(-0.17) 48	498 ^(+0.65) 191 ^(-0.98)	730 ^(-0.36) 142 ^(-1.20)	1079 ^(+0.34) 16 ^(+0.10)	0.59
$\tau_{\text{dif}}\infty, \Gamma_1 - 0.5$	42 ^(+0.68)	108 ^(+0.16)	311 ^(-0.34)	329 ^(+0.10) 56	519 ^(+1.59) 243 ^(+2.6)	744 ^(+0.15) 220 ^(+5.1)	1073 ^(+0.16) 31 ^(+3.7)	1.9
Dil. ($t_* > 7 \cdot 10^8$)	39 ^(+0.10)	114 ^(+0.74)	331 ^(+0.78)	323 ^(-0.21) 40	500 ^(+0.72) 206 ^(+0.21)	725 ^(-0.57) 164 ^(+0.59)	1071 ^(+0.09) 21 ^(+1.35)	0.49
$\Gamma_2 - 1.9$	45 ^(+1.1)	116 ^(+1.0)	322 ^(+0.29)	311 ^(-0.87) 40	491 ^(+0.30) 196 ^(-0.66)	691 ^(-1.8) 164 ^(+0.51)	1061 ^(-0.22) 23 ^(+1.65)	0.79
$\Gamma_2 - 2.0$	41 ^(+0.52)	125 ^(+1.9)	330 ^(+0.72)	331 ^(+0.22) 39	489 ^(+0.25) 205 ^(+0.00)	700 ^(-1.5) 162 ^(+0.43)	1087 ^(+0.58) 21 ^(+1.20)	0.64
$\Gamma_2 - 2.2$	34 ^(-0.58)	115 ^(+0.89)	322 ^(+0.30)	319 ^(-0.46) 45	503 ^(+0.87) 193 ^(-0.84)	727 ^(-0.48) 166 ^(+0.075)	1106 ^(+1.2) 23 ^(+1.8)	0.82
$\Gamma_2 - 2.3$	28 ^(-1.6)	112 ^(0.60)	317 ^(+0.01)	312 ^(-0.84) 43	505 ^(+0.97) 208 ^(+0.24)	764 ^(+0.90) 171 ^(+1.1)	1124 ^(+1.7) 21 ^(+1.3)	0.89
$\Gamma_1 - 1.60$	39 ^(+0.16)	123 ^(+1.7)	327 ^(+0.59)	331 ^(+0.24) 43	507 ^(+1.0) 204 ^(-0.04)	713 ^(-1.0) 159 ^(+0.19)	1107 ^(+1.2) 22 ^(+1.55)	0.66
$\Gamma_1 - 1.80$	41 ^(+0.45)	110 ^(+0.43)	315 ^(-0.11)	307 ^(-1.1) 46	479 ^(-0.23) 195 ^(-0.73)	727 ^(-0.46) 166 ^(+0.72)	1077 ^(+0.28) 23 ^(+1.7)	0.64
$\gamma 0.03$	38 ^(+0.03)	113 ^(+0.70)	326 ^(+0.52)	316 ^(-0.61) 43	479 ^(-0.22) 206 ^(+0.08)	709 ^(-1.1) 175 ^(+1.4)	1115 ^(+1.4) 20 ^(+0.91)	0.72
$\gamma 0.06$	38 ^(+0.03)	110 ^(+0.37)	318 ^(+0.04)	326 ^(-0.08) 46	478 ^(-0.26) 214 ^(+0.63)	721 ^(-0.69) 203 ^(+3.6)	1123 ^(+1.69) 25 ^(+2.3)	1.16

diagram. Instead, we used a random smearing prescription (see Schröder 1998) which would match the appearance of the observed HR diagram. It comprises the residual distance uncertainties in the Hipparcos parallaxes, photometric errors and some variation in metallicity.

Table 2 lists the characteristic star counts of different synthetic stellar samples, starting with the best match which we obtained with the simple diffusion approximation (model type a), when using an IMF with $\Gamma_1 = -1.65$ and $\Gamma_2 = -2.05$, an overshoot-onset (ovo) at $1.50M_{\odot}$ (see below) and a constant (genuine) SFR ($\gamma = 0.0$) in the volume. Obviously, this simplistic model gives the best *empirical* description of the depletion. Therefore, we use it as a reference for all other synthetic samples. In all our models (with the exceptions of $t_{9\text{max}}10$ and $t_{9\text{max}}8$, see below), star formation starts 9

billion years ago, which is a commonly adopted age of the thin galactic disk (Hernández et al, 2001).

– **Evaluation of match quality:** In order to decide the match quality of any synthetic sample on a quantitative scale, we compute the average ($|\delta|_{\text{av}}$, listed by the last column in Table 2) of all individual deviations from the observed star counts n_i , in units of their individual statistical variations $\sqrt{n_i}$. We prefer the choice of a simple (linear) average over the rms error because not all individual deviations are independent of each other. Also, a double weight has been given to the deviations of the age-sensitive KGC and LGB counts for balancing these with those of the seven MS counts. Of the observed complete sample, counts for MS6 and MS7 have been corrected for some incompleteness, see previous section. The synthetic star counts were obtained

from 5 times larger samples, to reduce their statistical contributions to the deviations.

Besides their average, the individual δ -values are equally important for the choices of best-matching parameter. In fact, each of the parameters discussed below affects only certain counts in a very specific way, while the corresponding change in $|\delta|_{\text{av}}$ appears to be much less significant. In this way, degeneracies with multiple parameter changes are avoided. In Table 2, we therefore highlighted individual mismatches by bold-face printing of the respective δ -value.

– **Onset of overshooting on the MS:** Because of the now larger (than in previous work) and therefore more critical star counts along the MS, we had first to reconsider the exact onset of MS overshooting by comparing the effects of different evolution grids on the MS star counts. For this comparison, we used the simple diffusion model because it would not introduce any artificial count-change along the MS (while the artificially abrupt onset of dilution at $t_* > 7 \cdot 10^8$ yrs in our model type (b) does, marginally so). The best match (i.e., lowest mean deviation of its star counts from the observed record) is then achieved with an overshoot-onset (ovo) at $1.50M_{\odot}$, see Table 2. This is in good agreement with Pols et al. (1998) but slightly different from our previous choice of $1.8M_{\odot}$.

By contrast, the star counts of synthetic samples computed with ovo = 1.8, ovo = 1.6, and ovo = 1.4 (all parameters for IMF and SFR left unchanged, i.e. $\Gamma_1 = -1.65$, $\Gamma_2 = -2.05$, $\gamma = 0.0$), show how a different onset point on the MS leaves systematic deviations from the observed MS star counts just above and below the onset, caused by the (then wrong) MS lifetimes of the corresponding stellar models. With hindsight, a mismatch in MS4, related to the use of an onset at $1.8 M_{\odot}$, can be noted in our earlier synthetic samples (Schröder & Sedlmayr 2001), but the much smaller observed $d < 50$ pc sample used then as a reference did not provide a precise-enough test on the MS overshoot-onset.

– **Age of the thin disk population:** We then made a comparison (again using the simple diffusion model) between synthetic samples computed for a different age of the “thin disk”. These are listed in Table 2 as models $t_{9\text{max}10}$ and $t_{9\text{max}8}$, where star formation starts 10^9 yrs earlier (see Binney et al. 2000 who argue for an older solar neighbourhood) and later. The resulting synthetic samples are not very sensitive to the exact value adopted for age of the thin disk. This can be understood, since the contribution of the earliest star formation to the present-day star counts is depleted by about a factor of 2.

– **Depletion description:** To demonstrate the importance of matching the depletion factors, we also list a synthetic sample without any depletion ($\tau_{\text{dif}} = \infty$), which models the solar neighbourhood (unrealistically) as a kind of “closed-box”. Despite a significant reduction in the IMF of the less massive (older) stars to match present-day star counts ($\Gamma_1 = -0.5$ instead of -1.65), it is impossible to match the observed numbers of evolved stars. These are much lower than those predicted by stellar evolution time-scales – clearly, a depletion is required which progresses with age.

See Fig. 2 for a plot of the depletion factor as a function of stellar age, compared to the reciprocal scale-height on an appropriately adapted scale ($1 = 1/195$ pc). Both curves coincide well for ages larger than $7 \cdot 10^8$ yrs, for which the dilution approach applies.

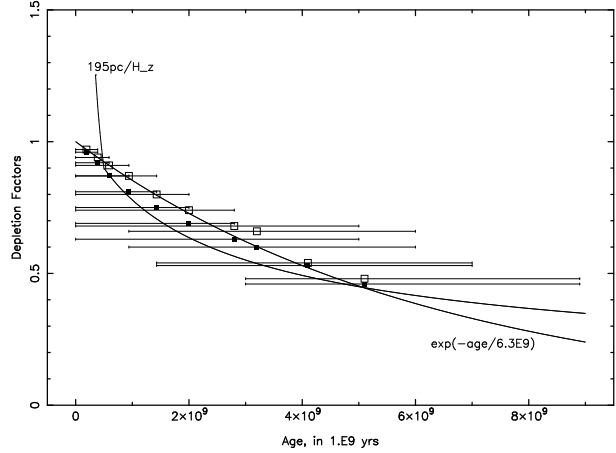


Figure 2. Empirical depletion factors, averaged over star groups listed in Table 3, with approximate age ranges indicated. Open squares: depletion according to model (a), filled squares: model (b). Shown for reference are the depletion prescriptions for individual age: the exponential depletion used by model (a), and the dilution ($\propto H_z^{-1}$) used by model (b) beyond the age required for thermalization and radial mixing ($t_* > 7 \cdot 10^8$ yrs).

Finally, Table 2 lists several samples with the above-described approach of a depletion by dilution. The entry of Dil. ($t_* > 0.7$ Gyr) represents the best match, obtained with $\Gamma_1 = -1.70$ and $\Gamma_2 = -2.10$ for the IMF and without any change over time of the genuine SFR ($\gamma = 0.0$) in the sample volume. Table 3 and Fig. 2 show that the actual depletion in the various groups of stars of this model are indeed very similar to those derived from the simplistic but well-matching diffusion approximation. The final synthetic samples in Table 2 demonstrate the sensitivity of the synthetic samples to changes in the parameters for IMF and SFR.

– **Cut-off for z-values:** We have also tested our anticipation that it would matter to select for stars with small z when deriving the IMF from a given volume in the galactic plane. For this purpose, we modelled the stellar content of the *whole* spherical volume in $d < 100$ pc, i.e., with the larger z -values included. The best match (not listed here) then indeed requires a much steeper IMF in its upper part, with $\Gamma_2 = -2.35$ ($\Gamma_1 = -1.75$), caused by the already significant drop in massive stars with increasing $|z|$.

– **Best matching IMF and SFR:** Table 4 summarises the properties of the IMF and SFR of the best matching synthetic samples. Despite their different approach to describe the depletion of the galactic plane, both models (a) and (b) result in a quite steep IMF with $\Gamma_1 = -1.7 \pm 0.1$ for $1.6M_{\odot} > M_* > \approx 1.1M_{\odot}$ and $\Gamma_2 = -2.1 \pm 0.1$ for $\approx 4M_{\odot} > M_* > 1.6M_{\odot}$.

Furthermore, we find a present star formation rate SFR(0) in the solar neighbourhood of about $3.2(\pm 0.1) \cdot 10^{-6}*/\text{yr}$ in a volume of $1.5 \cdot 10^6 \text{pc}^3$ centred on the galactic plane, which is 2.1 stars per 1000 years and $(\text{kpc})^3$. This value of the SFR applies only to the stars with a mass larger than $0.9M_{\odot}$. We cannot consider any less massive stars because these are not luminous enough to appear in any of the specific HRD regions counted here, nor would they have evolved into the giant branch yet.

In case there may have been a genuinely higher SFR

Table 3. Averaged properties (masses, ages, scale heights, depletion factors) with the simple diffusion approximation (a) and with stellar depletion by (mainly) dilution (b) for the synthetic stars of specific HRD regions (compare with Table 1).

	MS1	MS2	MS3	MS4	MS5	MS6	MS7	KGC	LGB	CW
$\langle M \rangle / M_{\odot}$	4.0	2.6	2.0	1.70	1.53	1.37	1.24	1.70	1.30	1.53
$\langle \text{Age} \rangle / \text{yrs}$	$1.9 \cdot 10^8$	$3.9 \cdot 10^8$	$5.9 \cdot 10^8$	$9.4 \cdot 10^8$	$1.43 \cdot 10^9$	$2.0 \cdot 10^9$	$2.8 \cdot 10^9$	$3.2 \cdot 10^9$	$5.1 \cdot 10^9$	$4.1 \cdot 10^9$
$\langle H_z \rangle / \text{pc}$	80	135	170	210	250	280	320	350	430	390
$F_{\text{depl}}(\text{a})$	0.97	0.94	0.91	0.87	0.80	0.74	0.68	0.66	0.48	0.54
$F_{\text{depl}}(\text{b})$	0.96	0.92	0.87	0.81	0.75	0.69	0.63	0.60	0.46	0.53

Table 4. Slope of IMF (Scalo notation) listed for the two best matching models (simple diffusion approximation and depletion by diffusion & dilution, see Table 2), both with constant SFR, and two less good matches using a SFR slightly higher in the past.

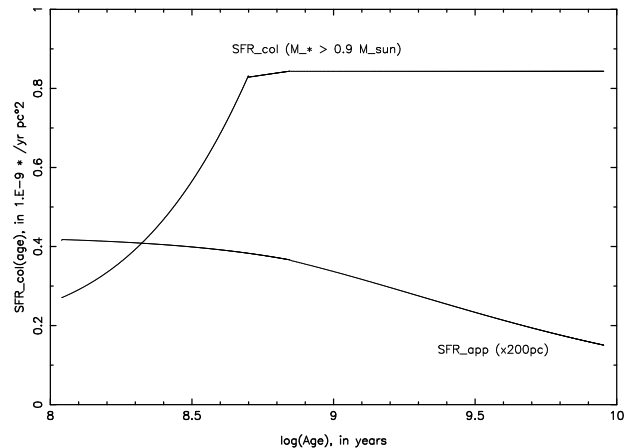
Depletion by	SFR(0)	γ	Γ_1	Γ_2	$ \delta _{\text{av}}$
$\tau_{\text{dif}} = 6.3 \cdot 10^9 \text{ yrs}$	$3.03 \cdot 10^{-6}$	0.00	-1.65	-2.05	0.30
Dil. ($t_* > 7 \cdot 10^8$)	$3.2 \cdot 10^{-6}$	0.00	-1.70	-2.10	0.49
Dil. ($t_* > 7 \cdot 10^8$)	$3.0 \cdot 10^{-6}$	0.03	-1.60	-2.00	0.72
Dil. ($t_* > 7 \cdot 10^8$)	$2.8 \cdot 10^{-6}$	0.06	-1.40	-2.00	1.16

in the past (9 billion years ago) on a 1.3 to 1.7 \times higher level (averaged radially and over a time-scale of a billion years), we tried models with $\gamma = 0.03$ and $\gamma = 0.06$, respectively. Such synthetic samples require a less steep IMF (see Table 4), but the over-all quality of the best match is systematically less good (larger $|\delta|_{\text{av}}$) than is achieved with the constant level of “thin disk” star formation. In particular, the count of the oldest group of stars (LGB) becomes significantly too large (see last lines in Table 2) when γ exceeds 0.03.

Finally, Fig. 3 shows the approximate star formation rate in the column (acc. to Equ. 15), as it appears from our observations in the volume in combination with our semi-empirical density scale-height as a function of age (Equ. 10, 11). As already mentioned, the column integral SFR_{col} grows by a factor of 4 from its low present-day (local, in-between spiral arms) value until it reaches an approximately constant, non-local disk-average of $0.82 \cdot \text{Gyr}^{-1} \text{pc}^{-2}$ for all stars older than about $7 \cdot 10^8 \text{ yrs}$ (and $M_* > 0.9 M_{\odot}$). Of these, a large fraction must have been collected by the present-day solar neighbourhood as a result of radial mixing. We would like to note that a sampling range on the kpc scale (like the one for luminous stars of Scalo, 1986) could not show such a pronounced effect. Rather, a large sample volume partly includes the neighbouring spiral arms and should show SFR_{col} values much nearer to the disk-average in the first place.

6 DISCUSSION AND OUTLOOK

In our approach to assess the local galactic “thin disk” IMF of single field stars by means of synthetic stellar samples which match the observed, complete (volume-limited) sample of solar neighbourhood stars, we have given special attention to three points vital to an unbiased IMF assessment: discrimination for stars near the galactic plane ($|z| < 25 \text{ pc}$),

**Figure 3.** Column-integrated SFR_{col} of the galactic disk over stellar age derived from our model (b), given in 10^{-9} stars per year and pc^2 , over $\log(\text{age})$. Note the apparent increase over the recent past ($t_* < 7 \cdot 10^8 \text{ yrs}$) where radial mixing changes the observed SFR from its low, local (interarm) value to a much larger (and fairly constant) non-local average. For reference, the apparent SFR in the local volume is also shown ($\times 200 \text{ pc}$). Its decline with age reflects the dilution of “thin disk” stars as they expand into larger scale-heights.

a realistic (semi-empirical) quantification of the stellar depletion in the galactic plane, and use of the specific, age-dependent information buried in the account of the evolved stars in the stellar sample.

Although we demonstrated that the simple approach of an age-independent diffusion time-scale, as used by us before (Schröder & Sedlmayr, 2001), does not yield too much different an IMF from the more sophisticated, semi-empirical depletion by diffusion and dilution, the IMF derived here supersedes our earlier work in several respects: (i) The present work is based on a much larger observed sample and yields significantly smaller error bars. (ii) The observed sample is a better representation of the stellar component in the immediate galactic plane, and (iii) the synthetic samples have now been created with a better choice of the onset of overshooting on the MS.

The slope of the field star IMF (i.e., $\Gamma_1 = -1.7$, $\Gamma_2 = -2.0$) obtained by this study for medium to high masses is remarkably similar to the range of values considered by Scalo (1986, 1998), despite being based on a very different approach. In principle, the genuine IMF and the depletion-corrected SFR in a defined volume on the galactic plane, as determined here, are equivalent to their column-integrated

quantities studied by the classical approach, in how they depend on mass and age. In fact, in our column-integrated quantities, a depletion by simple geometrical dilution must cancel with the growing scale height. At least, this is true for stars older than $7 \cdot 10^8$ yrs.

However, for stars younger than that, our column-integrated values are changing considerably, as demonstrated for the SFR by Fig. 3. This is the result of a progressive radial mixing into the small, local and inter-spiral-arm volume used here. For the respective stars (mainly, $M_* > 2M_\odot$) our column-integrated IMF would be unphysically steep. It does not compare to Scalo's (1986) IMF because his sampling range is about an order of magnitude larger. Also, he uses different scale heights for that range of young stars. Still, upon closer inspection (Pagel, 1997, p. 207), a slightly steeper slope ($\Gamma = -2.4$) does actually appear in the respective data of Scalo (1986). This may be due to the same effect (radial mixing – hence, not genuine), but much reduced by his vastly larger sampling scale. In any case, the slope of the lower mass IMF remains unaffected.

We see our approach of monte-carlo-created stellar samples, based on real evolution tracks and a good semi-empirical quantification of stellar depletion, compared one-to-one with an observed complete sample, as complementary to recently developed methods of inverting colour-magnitude diagrams with a maximum entropy method (see Hernández et al. 1999). While both methods make use of the *full* information content of the HR diagram, we find our approach is a very versatile tool and it may be more robust when studying the impact of more than one parameter.

Still, the above-mentioned problems with radial mixing and a very limited sampling-range make it difficult to deduce an exact slope of the galactic disk IMF for the more massive stars. In fact, we are unable to address the important question whether it may turn into a Salpeter dependence for the most massive stars (beyond about $6M_\odot$) which are important for the UV radiation field and any interaction with the ISM. Rather, the size of our observed sample is more limited than we would wish for. This is also true when it comes to the question of any genuine change of the SFR, or even the IMF, over time (see discussion by Kroupa 2001, e.g.). The results presented in the previous section provide, at best, support for an approximately constant SFR.

But these limitations will disappear as the situation is going to change dramatically in about a decade, when a new dimension of data, in a comfortably large sampling range, will become available with the above-mentioned projects GAIA and DIVA. Well tested, detailed models for creating synthetic stellar populations will then be a very powerful means of assessing the star formation history in our galaxy, and the depletion by dilution which provides a sensitive test of our understanding of galactic dynamics.

REFERENCES

Bastian U., Röser S., Hoeg E., Mandel H., et al. 1996, *Astron. Nachr.* 317, 281
 Bertelli G., Mateo M., Chiosi C., Bressan A., 1992, *ApJ* 388, 400
 Bertelli G., Nasi E. 2001, *ApJ* 121, 1013
 Binney J., Dehnen W., Bertelli G. 2000, *MNRAS* 318, 658
 Burkert A., Truran J.W., Hensler G. 1992, *ApJ* 391, 651
 Cohen M. 1995, *ApJ* 444, 874

Conti P.S., Vacca W.D. 1990, *AJ* 100, 431
 Dwek E. 1998, *ApJ* 501, 643
 Eggen O.J., Lynden-Bell D., Sandage A.R. 1962, *ApJ* 136, 748
 Eggleton P.P., 1971, *MNRAS* 151, 351
 Eggleton P.P., 1972, *MNRAS* 156, 361
 Eggleton P.P., 1973, *MNRAS* 163, 179
 Gilmore G., Reid I.N. 1983, *MNRAS* 202, 1025
 Gilmore G. 1999, *Ap&SS* 267, 109
 Hernández X., Valls-Gabaud D., Gilmore G. 1999, *MNRAS* 304, 705
 Hernández X., Avila-Reese V., Firmani C. 2001, *MNRAS* 327, 329
 Hensler G. 1999, *Ap&SS* 265, 397
 Jeans J.H. 1915, *MNRAS* 76, 71
 Jura M., Kleinmann S.G. 1992a, *ApJS* 79, 105
 Jura M., Kleinmann S.G. 1992b, *ApJS* 83, 329
 Jura M. 1994, *ApJ* 422, 102
 Kent S.M., Dame T.M., Fazio G. 1991, *ApJ* 378
 Kerber L.O., Javiel S.C., Santiago B.X. 2001, *A&A* 365, 424
 Kroupa P., Tout C.A., Gilmore G., 1991, *MNRAS*, 251, 293
 Kroupa P. 2001, *MNRAS* 322, 231
 Kuijken K., Gilmore G. 1989, *MN* 239, 605
 Lacey C. 1984, *MNRAS* 208, 687
 Layden, Andrew C. 1995, *AJ* 110, 2288
 Lynden-Bell D. 1962, *MNRAS* 124, 1
 Marsakov V.A., Shevelev Y.G. 1995, *AZ* 72, 630
 Mendez R.A., van Altena W.F. 1996, *AJ* 112, 665
 Miller G.E., Scalo J.M. 1979, *ApJS* 41, 513
 Oestreicher M.O., Schmidt-Kaler T. 1995, *A&A* 294, 57
 Ojha D.K., Bienaymé O., Robin A.C., Créze M., Mohan V. 1996, *A&A* 311, 456
 Ojha D.K., Bienaymé O., Mohan V., Robin A.C. 1999, *A&A* 351, 945
 Oort, J.H. 1932, *Bull. Astr. Inst. Netherlands* 6, 249
 Pagel B.E.J. 1997, in "Nucleosynthesis and Chemical Evolution of Galaxies", CUP, Cambridge
 Pagel B.E.J. 2001a, in "Cosmic Evolution", Vangioni-Flam E., Ferlet R., Lemoine M (eds.), New Jersey: World Scientific, 223
 Pagel B.E.J. 2001b, *PASP* 113, 137
 Perryman M.A.C., Lindegren L., Kovalevsky J., Høg E., Bastian U., et al. 1997, *A&A* 323, L49
 Perryman M.A.C. 2002, *Ap&SS* 280, 1
 Phleps S., Meisenheimer K., Fuchs B., Wolf C. 2000, *A&A* 356, 108
 Pilyugin L.S. 1996, *A&A* 313, 803
 Pols O.R., Tout C.A., Schröder K.-P., Eggleton P.P., Manners J. 1997, *MNRAS*, 289, 869
 Pols O.R., Schröder K.-P., Hurley J.R., Tout C.A., Eggleton P.P. 1998, *MNRAS*, 298, 525
 Reed B.C., 2000, *AJ* 120, 314
 Robin A.C., Haywood M., Créze M., Ojha D.K., Bienaymé O. 1996, *A&A* 305, 125
 Scalo J.M. 1986, *Fundam. Cosmic Phys.* 11, 1
 Scalo J.M. 1998, in "The Stellar Initial Mass Function", ASP Conf. Series 142, Gilmore G., Howell D. (eds.), 201
 Schröder K.-P., Pols O.R., Eggleton P.P. 1997, *MNRAS* 285, 696
 Schröder K.-P. 1998, *A&A* 334, 901
 Schröder K.-P., Sedlmayr E. 2001, *A&A* 366, 913
 Seifert W., Mandel H., Wagner S., Bastian U., Roeser S. 1998, *SPIE* 3356, 904
 Siebert A., Bienaymé O., Soubiran C. 2002, *A&A*, in print
 Sommer-Larsen J., Antonuccio-Delugo V. 1993, *MNRAS* 262, 350
 Vergely J.-L., Ferrero R.F., Egret D., Köppen J. 1998, *A&A* 340, 543
 Wielen R. 1977, *A&A* 60, 263